

1 GenNet framework: interpretable neural 2 networks for phenotype prediction 3

4 Arno van Hilten¹, Steven A. Kushner², Manfred Kayser³, M. Arfan Ikram⁴, Hieab H.H.

5 Adams^{1,5}, Caroline C.W. Klaver^{4,6}, Wiro J. Niessen^{*1,7} and Gennady V. Roshchupkin^{*1,4}

6 ¹ Department of Radiology and Nuclear Medicine, Erasmus MC, Medical Center, Rotterdam, the
7 Netherlands.

8 ² Department of Psychiatry, Erasmus MC, Medical Center, Rotterdam, the Netherlands.

9 ³ Department of Genetic Identification, Erasmus MC, Medical Center, Rotterdam, the
10 Netherlands.

11 ⁴ Department of Epidemiology, Erasmus MC, Medical Center, Rotterdam, the Netherlands.

12 ⁵ Department of Clinical Genetics, Erasmus MC, Medical Center, Rotterdam, the Netherlands.

13 ⁶ Department of Ophthalmology, Erasmus MC, Medical Center, Rotterdam, the Netherlands.

14 ⁷ Faculty of Applied Sciences, TU Delft, Delft, the Netherlands.

15
16 *Jointly supervised this project
17

18 **Neural networks have been seldomly leveraged in population genomics due to the**
19 **computational burden and challenge of interpretability. Here, we propose GenNet, a novel**
20 **open-source deep learning framework for predicting phenotype from genotype. In this**
21 **framework, public prior biological knowledge is used to construct interpretable and**
22 **memory-efficient neural network architectures. These architectures obtain good predictive**
23 **performance for multiple traits and complex diseases, opening the door for neural**
24 **networks in population genomics.**

25

26 **Introduction**

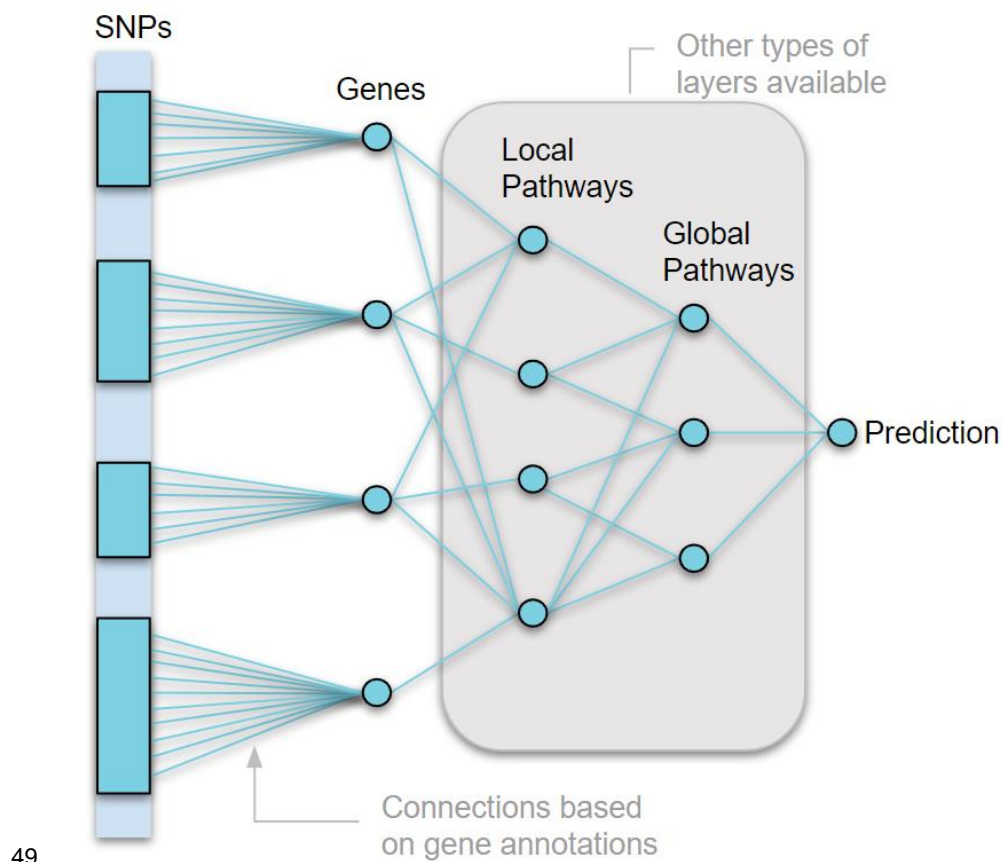
27 Genome-wide association studies (GWAS) have identified numerous genomic loci associated
28 with complex (polygenic) human traits and diseases. Recent GWAS studies with increasingly
29 larger sample sizes are leading to more significant associations between genotypes and

30 phenotypes at more and more independent loci. To illustrate, the latest GWAS for body height
31 based on 700,000 individuals identified more than 3000 near-independent significantly
32 associated single nucleotide polymorphisms (SNPs)¹. This information, used in combination with
33 annotated biological databases such as: NCBI RefSeq, KEGG, Reactome and GTEx has proven
34 to be highly valuable for understanding the underlying biological mechanisms of complex
35 diseases²⁻⁶. In this paper, we propose a new framework, GenNet, that integrates these biological
36 data sources for discovery and interpretability in an end-to-end deep learning framework for
37 predicting phenotypes.

38 Deep learning is the state of the art in many domains such as medical image analysis and natural
39 language processing because of its flexibility and modeling capabilities^{7,8}. In many cases, deep
40 learning yields better performance compared to traditional approaches, since it can model highly
41 non-linear relations and scales very well with data size. However, this often comes at the cost of
42 interpretability, since there is a trade-off between complexity and interpretability^{9,10}.

43 Additionally, when it comes to genotype data, the number of learnable parameters increases
44 dramatically because of the large input size, making it infeasible to use classical neural networks
45 in this domain. To overcome previous limitations, we propose a new framework, GenNet, in
46 which different types of biological information are used to define biologically plausible neural
47 network architectures, avoiding this trade-off and creating interpretable neural networks for

48 predicting complex phenotypes.



49

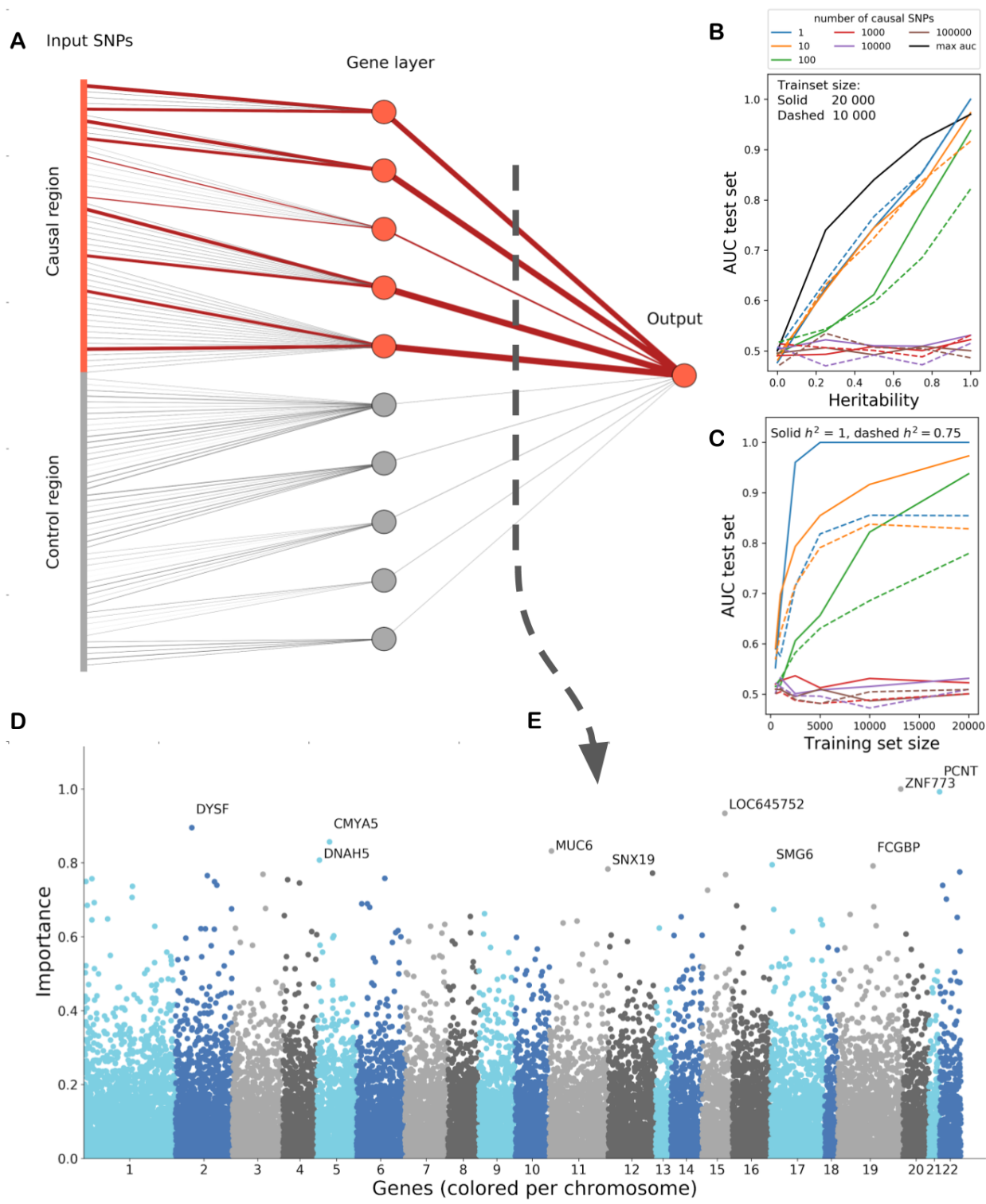
50 *Figure 1. Overview of the GenNet Framework. Neural networks are made by combining layers*
51 *made of different sources of prior biological knowledge (i.e. a gene layer from gene annotations,*
52 *a pathway layer from KEGG pathway annotations). These sources define the connections and*
53 *therefore the architecture, creating interpretable networks in the process.*

54

55 **Methods**

56 The main concept of the GenNet framework is summarized graphically in Figure 1. In this
57 framework, prior knowledge is used to create groups of connected nodes to reduce the number of
58 learnable parameters in comparison to a fully connected neural network. For example, in the first
59 layer, where biological knowledge in the form of gene annotations, is used to group millions of

60 single nucleotide polymorphisms (SNPs) and to connect those SNPs to their corresponding
61 genes. The resulting layer retains only meaningful connections, significantly reducing the total
62 number of parameters compared to a classical layer. As a result, these memory-efficient
63 networks are able to handle the millions of inputs needed for genotype-to-phenotype prediction.
64 The biological knowledge is thus used to define only meaningful connections, shaping the
65 architecture of the neural network. Interpretability is inherent to the neural network's
66 architecture. For example, a network that connects SNPs-to-genes and genes-to-output. The
67 learned weights of the connections between layers represent the effect of the SNP on the gene or
68 the effect of the gene on the output. In the network, all neurons represent thus biological entities
69 and weights model the effects between these entities, together forming a biologically
70 interpretable neural network. Each connection in the network is thus based on a biological
71 annotation and the learned weight for this connection represents the importance of this
72 annotation for the predicted outcome.
73 Many types of layers can be created using this principle. These layers can be used like building
74 blocks to form new network architectures. Apart from gene annotations, our framework provides
75 layers built from exon annotations, pathway annotations, chromosome annotations and cell and
76 tissue type expressions.



78 *Figure 2. A) Non-linear simulation showing the basic principle of the network, thickness of the*
 79 *connections represents the learned weight (causal, contributing connections in red, control*

80 *connections in grey). This proof of concept can be run online see <https://tinyurl.com/y8hh8rul>*
81 *(or see Supplementary 1.1). B) A secondary set of simulations show the performance of GenNet,*
82 *expressed in the area under the curve, for increasing levels of heritability and training set size*
83 *(C). In black the theoretical maximum of the AUC versus heritability¹¹. D) Manhattan plot of the*
84 *importance of the genes according to the network for distinguishing between schizophrenia cases*
85 *and controls. E) This Manhattan plot is a cross section between the gene layer and the outcome*
86 *of the trained network.*

87

88 **Results**

89 In order to evaluate the network's performance under a variety of conditions, synthetic data was
90 created with different levels of heritability, number of training samples and polygenicity (see
91 Supplementary Materials 1 for results and detailed description). Figure 2A shows the proof of
92 concept demo that can be run online. Figure 2B and 2C show the main trends in the simulations.
93 As would be expected, the network performs best for traits with high heritability, high number of
94 training samples and low polygenicity, and the performance decreases with decreasing
95 heritability, number of training samples or increase of polygenicity.

96 Motivated by the proof of concept and the outcomes of the simulations, the framework was
97 applied to real data from multiple sources, including population-based data from the UK Biobank
98 study and the Rotterdam study, and a case-controls study on schizophrenia from Sweden¹²⁻¹⁴.
99 The analyzed phenotypes vary from traits where high predictive performance can be obtained
100 from a dozen of variants (eye color) to disorders where thousands of variants only explain a
101 small portion of the variance (schizophrenia and bipolar disorder)^{15,16}. The genotype data
102 employed included imputed microarray-based GWAS data (eye color in Rotterdam study) as

103 well as whole exome sequencing (WES) data (hair color, male baldness pattern and bipolar
 104 disorder in UK Biobank; schizophrenia in the Swedish study). An overview of the experiments
 105 and results can be found in table 1.

Trait	Dataset (type)	Number of input variants	Subjects & phenotype		Heritability	AUC LASSO	AUC GenNet	GenNet: top three most important genes
			Class I	Class II				
Eye color	Rotterdam (genotype array)	113,241 (exonic) inputs of 16,628 genes	4041 Blue	2250 Other	0.80-0.98	0.68	0.75	<i>HERC2</i> , <i>OCA2</i> , <i>LAMC1</i>
Hair color	UK Biobank (exome)	6,986,636 input variants of 15,827 genes	1648 Blond	1656 Red	0.70-0.97	0.78	0.83	<i>MCIR</i> [*] , <i>OCA2</i> , <i>TC2N</i>
			1672 Dark brown	1664 Red	0.70-0.97	0.79	0.88	<i>MCIR</i> [*] , <i>OCA2</i> , <i>ZCCHC4</i>
			4352 Blond	4343 Dark Brown	0.70-0.97	0.64	0.75	<i>OCA2</i> , <i>TC2N</i> , <i>EXOC2</i>
Male baldness	UK Biobank (exome)	6,986,636 Input variants of 15,827 genes.	3454 No balding	3454 Severe balding	0.60-0.70	0.57	0.57	<i>NGEF</i> , <i>NKRD18B</i> , <i>SYNJ2</i>
Bipolar	UK Biobank (exome)	6,986,636 Input variants of 15,827 genes	343 Cases	347 Controls	0.73-0.93	0.59	0.60	<i>LINC00266-1</i> , <i>CSMD1</i> , <i>TCERG1L</i>
Schizophrenia	Sweden (exome)	1,288,701 input variants of 21,390 genes	4969 Cases	6245 Controls	0.80-0.85	0.65	0.74	<i>ZNF773</i> , <i>PCNT</i> , <i>DYSF</i>

106 *Table 1. Summary of the experiments and results in this study for the simplest network in our
 107 framework that contains the input SNPs, the gene layer and the output layer. Manhattan plots for
 108 gene importance can be found in Supplementary Materials 2,3 & 4. *MCIR was not present in
 109 gene annotations but was identified by linkage disequilibrium.*

110
 111 In general, the framework's predictive performance is in line with trends seen in simulations and
 112 literature. Phenotypes with more training samples and phenotypes that require less variants to
 113 obtain good predictive performance, such as eye and hair color, performed best. Nonetheless, a
 114 good predictive performance, area under curve (AUC) of 0.74 in the held-out test set, was

115 obtained for schizophrenia, a highly polygenic disorder. All models outperform or match the
116 baseline LASSO logistic regression model (see Methods).

117 Inspecting the networks, we found that the *OCA2* gene was highlighted as the most important
118 gene to distinguish between brown and blond hair color. *OCA2* is involved in the transport of
119 tyrosine, a precursor of melanin¹⁷. The signal is probably amplified by the nearby *HERC2*,
120 previous identified via functional genetic studies as harboring a strong, long-distance enhancer
121 regulating *OCA2* gene expression to cause pigmentation variation¹⁷. *OCA2* and *HERC* are the
122 two most predictive genes according to the network for predicting blue (iris) eye color. Both
123 have been earlier identified by hair and eye color GWASes¹⁸⁻²⁰.

124 In the experiments with schizophrenia as outcome, the network was able to classify cases and
125 controls with a maximum accuracy of 68.4% (mean of 66.3 ± 1.37 over 10 runs). We estimate
126 the theoretical upper limit for classification, including all genetic aspects, to be an accuracy of
127 72% (supplementary methods 5). The model obtains an area under the receiver operating curve
128 of 0.74 (ranging 0.72-0.74) in the held-out test set, thereby considerably outperforming the
129 LASSO logistic regression baseline (AUC of 0.64). The GenNet AUC compares favorably to
130 polygenic risk scoring for schizophrenia, which have AUC values on the order of 0.70 (ranging
131 0.49-0.85)¹⁵. This is noteworthy since in this study the schizophrenia predictions are based on
132 whole exome sequencing data as opposed to GWAS arrays spanning the whole genome.

133

134

135 **Discussion**

136 Here, we present a novel framework to train interpretable neural networks for phenotype
137 prediction from genotype. The proposed neural networks have connections defined by prior
138 biological knowledge only, reducing the number of connections and therefore the number of

139 trainable parameters. Consequently, the networks are interpretable and overcome computational
140 limitations. All experiments were run on a single GPU (Nvidia GeForce GTX 1080) and
141 converged within 48 hours. Simulations show the network's performance when varying the
142 degree of heritability, polygenicity and sample size. The suggested sample size, heritability and
143 polygenicity are conservative. When applying the framework to UK Biobank, Rotterdam study
144 and Swedish Schizophrenia WES data, good predictive performance was achieved with smaller
145 sample sizes and higher number of inputs than suggested by the simulations. In these
146 experiments, widely different phenotypes are predicted with generally good performance based
147 exclusively on WES SNPs.

148 For traits with a known etiology, well-replicated genes such as *HERC2* and *OCA2* for eye color
149 and *OCA2* and *TCN2* for hair color were found to be important by the network¹⁸⁻²¹. For
150 schizophrenia, a disorder with an unclear etiology, the network identified previously
151 unimplicated genes, including *ZNF773* and *PCNT*. However, it is important to note that the
152 importance captured by the network bears more similarity to effect size rather than statistical
153 significance.

154 In general, these experiments indicate that neural networks in our framework can overcome
155 computational limitations while still obtaining good predictive performance, opening the door for
156 genetic risk prediction by neural networks. Aside from computational benefits, the architecture
157 offers interpretability, alleviating one the most important shortcomings of neural networks. In
158 this study, WES data and exonic variants from microarrays have been used, however the
159 principles in the GenNet framework can be leveraged to handle diverse types of input, including
160 genotype, gene expression and methylation data or combinations thereof)

161

162

163 In conclusion, we developed a freely-available framework, which can be used to build
164 interpretable neural networks for genotype data by incorporating prior biological knowledge. We
165 have demonstrated the effectiveness of this novel framework across multiple datasets and for
166 multiple phenotypes. Given that each network node is interpretable, we anticipate this approach
167 to have wide applicability for uncovering novel insights into the genetic architecture of complex
168 traits and diseases.

169

170 GenNet is an open-source framework, providing code and tutorials
171 (<https://github.com/arnovanhilten/GenNet/>). This includes tutorials for applying the networks as
172 well as creating new layers and networks from prior knowledge.

173

174

175 **Online Methods**

176 **Sweden Schizophrenia**

177 Sweden-Schizophrenia Population-Based Case-Control Exome Sequencing study (dbGaP
178 phs000473.v2.p2), is a case control study with 4969 cases and 6245 controls¹⁴. All individuals
179 aged 18-65, have parents born in Sweden and provided written informed consent. Cases were at
180 least 2 times hospitalized with schizophrenia discharge diagnosis and do not have a hospital
181 register diagnosis consistent with a medical or other psychiatric disorder that mitigates the
182 schizophrenia diagnosis. Cases do not have a relationship closer than 2nd degree relative with
183 any other case. Controls do not have any relation to either case or control and all controls have
184 never been hospitalized with a discharge diagnosis of schizophrenia.

185 The .bim, .bam and .bed files were converted using HASE²² to .h5 format, a format that allows
186 fast and parallel data reading. After conversion, the data is transposed and SNPs without any
187 variance are removed (~1.2 million SNPs remain). The data is split in a training, validation and
188 test set (ratio of 60/20/20), while preserving the ratio cases and controls. All SNPs with standard
189 deviation greater than zero are used as input to the network after z-score normalization (based on
190 the mean and standard deviation of the training set).

191

192 **UK Biobank**

193 We applied the framework to multiple phenotypes in the UK Biobank using the first release of
194 the WES data, providing whole exome sequencing for 50,000 UK Biobank participants²³.
195 Phenotypes are self-reported (touchscreen questions UK Biobank Assessment Centre). Similar to
196 the Sweden cohort all variants without variance were removed, data was converted to
197 hierarchical data format (.h5), and transposed. For every phenotype an equal number of cases

198 and controls were sampled. The resulting dataset is split in a train, validation and a test set (ratio
199 of 60/20/20). Related cases, and cases with related controls, (kinship > 0.0625) are all in the
200 training set. This is done under the assumption that related cases and controls could ease training,
201 the shared genetic information could steer the network towards the discriminatory features. The
202 validation and test sets contain only unrelated cases and controls within and between sets.
203 Unrelated controls are randomly sampled and added to gain an even distribution between cases
204 and controls in all sets. Misaligned SNPs and sex chromosomes were masked in the first layer
205 and therefore not included in the study.

206

207 **Rotterdam Study**

208 The Rotterdam study is a prospective cohort study, in the first cohort 6291 participants were
209 genotyped using the Illumina 550K and 550K duo arrays. Samples with low call rate (<97.5%),
210 with excess autosomal heterozygosity (>0.336) or with sex-mismatch were excluded, as were
211 outliers identified by the identity-by-state clustering analysis (outliers were defined as being >3
212 standard deviation (SD) from population mean or having identity-by-state probabilities >97%).
213 For imputation the Markov Chain Haplotyping (MACH) package version 1.0 software (Imputed
214 to plus strand of NCBI build 37, 1000 Genomes phase I version 3) and minimac version 2012.8.6
215 were used (call rate >98%, MAF >0.001 and Hardy–Weinberg equilibrium P-value > 10⁻⁶).

216 From here on processing steps are identical as described for Sweden Schizophrenia obtaining
217 113,241 exonic variants.

218 Eyes were examined by an ophthalmological medical researcher and eye (iris) color was
219 categorized into three categories; blue, intermediate and brown using standard images and based
220 on the predominant color and pigmentation ²⁴.

221

222 **Prior Knowledge**

223 All SNPs were annotated using Annovar²⁵. A sparse connectivity matrix is generated connecting
224 the SNPs to their corresponding genes. The intron-exon annotations of Annovar were used as a
225 proxy to create the connectivity matrices between SNPs, exons and genes. The pathway masks
226 were built by using GeneSCF²⁶ and the KEGG database³. GTEx tissue-expression masks were
227 made using the fully processed, filtered and normalized gene expression matrices for each tissue
228 directly obtainable from the GTEx website⁵ and from derived t-score statistics²⁷. Single cell
229 expression masks are available made using data from FUMA²⁸. Expression masks are continuous
230 and various thresholds can be used to create connectivity matrices, the threshold should be
231 chosen with care to ensure unique nodes and thus interpretability.

232 All available networks in the framework are trait independent but trait specific neural networks
233 can be created with more specific prior knowledge (e.g. brain cell expression to select genes in
234 the network for predicting neurological disorders). The GenNet framework is quite flexible, any
235 information that groups data uniquely can be used to create layers.

236

237 **Neural Network Architecture**

238 In the GenNet framework, layers are available built from biological knowledge such as; exon
239 annotations, gene annotations, pathway annotations, cell expression and tissue expression.
240 Information from these resources are used to define only meaningful connections, shaping an
241 interpretable and lightweight neural network, allowing evaluation of millions of input variants
242 together. These networks bear similarities to the first generation of neural networks and recently
243 interest for these networks has rekindled for biological applications²⁹⁻³², In neural networks the

244 dimensionality of the data is reduced, resulting in a loss of information every layer. Networks
245 with the GenNet architecture aim to reduce this loss by using prior biological knowledge to
246 create layers in the network, compressing the network in a biologically sensible way. These
247 sources are used to define connections between nodes/neurons in the network (see
248 implementation). The network itself will learn how important the connections are for the
249 prediction of the outcome. Thus, giving additional information for the sources used to define the
250 network. For example, in most networks, gene annotations are used to group SNPs. During
251 training the network will figure out which gene is important and which SNPs in the gene are
252 important for predicting the outcome.

253

254 **Interpretation**

255 Interpretation of the network is straightforward due to the simplicity of the concept, the higher
256 the weight is the more important it is for the network. A network built by gene annotations can
257 be seen as ~20 000 (number of genes) parallel regressions followed by a single logistic
258 regression. The learned weights in these regressions are similar to the coefficients in logistic
259 regression. Especially the last node, a single neuron with a sigmoid activation, $P =$
260 $\text{Sigmoid}(\sum_{i=0}^n x_i w_i + B)$ is similar to logistic regression $Y = \text{Sigmoid}(\sum_{i=0}^n x_i \beta_i + B)$.
261 To compare coefficients (β) the inputs are normalized in logistic regression. In the neural
262 network this is achieved by batch normalization (without center and scaling), normalizing the
263 weights (w) after every activation. Since batch normalization is a batch-wise approximation the
264 learned weights can be multiplied with the standard deviation of the activations for a more
265 accurate estimate, resulting in the importance measure. We noticed it might be beneficial to add
266 an L1 penalty on the weights in the last dense layer, as used in LASSO logistic regression. This

267 regularizer constraints the search space which might lead to a better generalization and reduced
268 noise in the signal for easier interpretation.

269

270 **Implementation**

271 Technically, the computational performance of the implemented Keras/Tensorflow^{33,34} layer
272 should be on par or an improvement over similar layers. It is implemented using sparse matrix
273 multiplication, making it faster than the slice-wise locallyconnected1D layer and more memory
274 efficient than dense matrix multiplication. The layer is friendly to use, with only one extra input
275 compared to a normal dense layer. This extra input, the sparse connectivity matrix, is made with
276 prior knowledge and describes how neurons are connected between layers.

277 The networks behave similar to normal fully connected artificial neural networks but is pruned
278 by removing irrelevant connection ($Out = Activation(\sum_{i=0}^n x_i w_i + b)$) With w as a sparse
279 matrix with learnable weights, initialized with a sparse connectivity matrix defining connections.
280 The networks are optimized using the ADAM or Adadelta optimizers^{35,36}, using weighted binary
281 cross entropy with weights depending on the imbalance of the classes, and are all trained on a
282 single GPU.

283

284 **Baseline**

285 As a baseline method, LASSO logistic regression was implemented in Tensorflow by using a
286 dense layer of a single neuron with a sigmoid activation function and L1 regularization on
287 weights.

288

289 **Upper Bound**

290 Population characteristics can be used to calculate the upper bound of performance for a
291 classifier for any trait. This can be done by creating a confusion matrix. The accuracy between
292 true and false positives for a perfect classifier, based solely on genetic inputs, is given by the
293 concordance rate between monozygotic twins. It is impossible to predict better based solely on
294 genetic code than the rate a trait occurs in people with virtually the same genetic code. The
295 chance of misclassifying a control should be better than the prevalence, which is often close to
296 zero for most diseases. Creating a confusion matrix can give insights in the upper bound for
297 accuracy, sensitivity and specificity in the dataset. An example for schizophrenia in our dataset
298 can be found in Supplementary 5.

299

300 **Code Availability**

301 The code, tutorials and trained networks can be found on github.com/arnovanhilten/GenNet/ in
302 the form of Jupyter notebooks. The code has been made with an emphasis on easy to use, with
303 comments and tutorials.

304

305 **Data Availability**

306 Code to run and generate data for the simulations are publicly available on GitHub. The genetic
307 and phenotypic UK Biobank data are available upon application to the UK Biobank
308 (<https://www.ukbiobank.ac.uk/>). Access to the Sweden-Schizophrenia Exome Sequencing study
309 can be requested on DBGaP (<https://www.ncbi.nlm.nih.gov/gap/>) (dbGaP phs000473.v2.p2).

310

311 **References**

312

313 1. Yengo L, Sidorenko J, Kemper KE, et al. Meta-analysis of genome-wide association studies for height and
314 body mass index in~ 700000 individuals of European ancestry. *Human Molecular Genetics*.
315 2018;27(20):3641-3649.

316 2. Pruitt KD, Tatusova T, Maglott DR. NCBI reference sequences (RefSeq): a curated non-redundant
317 sequence database of genomes, transcripts and proteins. *Nucleic Acids Research*. 2007;35(suppl_1):D61-
318 D65.

319 3. Kanehisa M, Goto S. KEGG: kyoto encyclopedia of genes and genomes. *Nucleic Acids Research*.
320 2000;28(1):27-30.

321 4. Croft D, Mundo AF, Haw R, et al. The Reactome pathway knowledgebase. *Nucleic Acids Research*.
322 2014;42(D1):D472-D477.

323 5. Lonsdale J, Thomas J, Salvatore M, et al. The genotype-tissue expression (GTEx) project. *Nature Genetics*.
324 2013;45(6):580.

325 6. Gallagher MD, Chen-Plotkin AS. The post-GWAS era: from association to function. *The American Journal of
326 Human Genetics*. 2018;102(5):717-730.

327 7. Litjens G, Kooi T, Bejnordi BE, et al. A survey on deep learning in medical image analysis. *Medical Image
328 Analysis*. 2017;42:60-88.

329 8. Young T, Hazarika D, Poria S, Cambria E. Recent trends in deep learning based natural language
330 processing. *IEEE Computational Intelligence Magazine*. 2018;13(3):55-75.

331 9. Edwards L, Veale M. Slave to the algorithm: Why a right to an explanation is probably not the remedy you
332 are looking for. *Duke L & Tech Rev*. 2017;16:18.

333 10. Došilović FK, Brčić M, Hlupić N. Explainable artificial intelligence: A survey. Paper presented at: 2018 41st
334 International convention on information and communication technology, electronics and microelectronics
335 (MIPRO)2018.

336 11. Wray NR, Yang J, Goddard ME, Visscher PM. The genetic interpretation of area under the ROC curve in
337 genomic profiling. *PLoS genetics*. 2010;6(2).

338 12. Bycroft C, Freeman C, Petkova D, et al. The UK Biobank resource with deep phenotyping and genomic
339 data. *Nature*. 2018;562(7726):203-209.

340 13. Ikram MA, Brusselle G, Ghanbari M, et al. Objectives, design and main findings until 2020 from the
341 Rotterdam Study. *European Journal of Epidemiology*. 2020;1-35.

342 14. Genovese G, Fromer M, Stahl EA, et al. Increased burden of ultra-rare protein-altering variants among
343 4,877 individuals with schizophrenia. *Nature neuroscience*. 2016;19(11):1433.

344 15. Ripke S, Neale BM, Corvin A, et al. Biological insights from 108 schizophrenia-associated genetic loci.
345 *Nature*. 2014;511(7510):421-427.

346 16. Stahl EA, Breen G, Forstner AJ, et al. Genome-wide association study identifies 30 loci associated with
347 bipolar disorder. *Nature Genetics*. 2019;51(5):793-803.

348 17. Visser M, Kayser M, Palstra R-J. HERC2 rs12913832 modulates human pigmentation by attenuating
349 chromatin-loop formation between a long-range enhancer and the OCA2 promoter. *Genome Research*.
350 2012;22(3):446-455.

351 18. Han J, Kraft P, Nan H, et al. A genome-wide association study identifies novel alleles associated with hair
352 color and skin pigmentation. *PLoS genetics*. 2008;4(5).

353 19. Hysi PG, Valdes AM, Liu F, et al. Genome-wide association meta-analysis of individuals of European
354 ancestry identifies new loci explaining a substantial fraction of hair color variation and heritability. *Nature
355 Genetics*. 2018;50(5):652-656.

356 20. Candille SI, Absher DM, Beleza S, et al. Genome-wide association studies of quantitatively measured skin,
357 hair, and eye pigmentation in four European populations. *PloS One*. 2012;7(10).

358 21. Liu F, van Duijn K, Vingerling JR, et al. Eye color and the prediction of complex phenotypes from genotypes.
359 *Current Biology*. 2009;19(5):R192-R193.

360 22. Roshchupkin GV, Adams H, Vernooij MW, et al. HASE: Framework for efficient high-dimensional
361 association analyses. *Scientific Reports*. 2016;6:36076.

362 23. Van Hout CV, Tachmazidou I, Backman JD, et al. Whole exome sequencing and characterization of coding
363 variation in 49,960 individuals in the UK Biobank. *BioRxiv*. 2019:572347.

364 24. Kayser M, Liu F, Janssens ACJ, et al. Three genome-wide association studies and a linkage analysis
365 identify HERC2 as a human iris color gene. *The American Journal of Human Genetics*. 2008;82(2):411-423.

366 25. Wang K, Li M, Hakonarson H. ANNOVAR: functional annotation of genetic variants from high-throughput
367 sequencing data. *Nucleic Acids Research*. 2010;38(16):e164-e164.

368 26. Subhash S, Kanduri C. GeneSCF: a real-time based functional enrichment tool with support for multiple
369 organisms. *BMC Bioinformatics*. 2016;17(1):365.

370 27. Finucane HK, Reshef YA, Anttila V, et al. Heritability enrichment of specifically expressed genes identifies
371 disease-relevant tissues and cell types. *Nature genetics*. 2018;50(4):621-629.

372 28. Watanabe K, Mirkov MU, de Leeuw CA, van den Heuvel MP, Posthuma D. Genetic mapping of cell type
373 specificity for complex traits. *Nature communications*. 2019;10(1):1-13.

374 29. Gazestani VH, Lewis NE. From genotype to phenotype: Augmenting deep learning with networks and
375 systems biology. *Current Opinion in Systems Biology*. 2019.

376 30. Ma J, Yu MK, Fong S, et al. Using deep learning to model the hierarchical structure and function of a cell.
377 *Nature Methods*. 2018;15(4):290.

378 31. Michael KY, Ma J, Fisher J, Kreisberg JF, Raphael BJ, Ideker T. Visible machine learning for biomedicine.
379 *Cell*. 2018;173(7):1562-1565.

380 32. Wang D, Liu S, Warrell J, et al. Comprehensive functional genomic resource and integrative model for the
381 human brain. *Science*. 2018;362(6420):eaat8464.

382 33. Keras [computer program]. 2015.

383 34. Abadi M, Barham P, Chen J, et al. Tensorflow: A system for large-scale machine learning. Paper presented
384 at: 12th {USENIX} Symposium on Operating Systems Design and Implementation ({OSDI} 16)2016.

385 35. Zeiler MD. Adadelta: an adaptive learning rate method. *arXiv preprint arXiv:12125701*. 2012.

386 36. Kingma DP, Ba J. Adam: A method for stochastic optimization. *arXiv preprint arXiv:14126980*. 2014.

387

388 **Acknowledgements**

389 This work was funded by the Dutch Technology Foundation (STW) through the 2005 Simon
390 Steven Meester grant 2015 to W.J. Niessen. This research has been conducted using the UK
391 Biobank Resource under Application Number 23509. This work was carried out on the Dutch
392 national e-infrastructure with the support of SURF Cooperative (application number 17610). The
393 Rotterdam study is supported by the Netherlands Organization for Scientific Research (NWO,
394 91203014, 175.010.2005.011, 91103012).

395

396 **Author contributions**

397 A.H and G.R conceived and designed the method. A.H performed experiments and implemented
398 the method. G.R and W.N supervised the work. M.A.I, C.K, H.A, M.K and S.K. provided or
399 gave access to data. A.H, G.R, W.N, M.K., M.A.I., S.K, wrote, re-vised and approved the
400 manuscript.

401

402 **Competing interests**

403 W. N. is co-founder and shareholder of Quantib BV. Other authors declare no competing
404 interests.

405

406 **Additional Information**

407 Supplementary is available for this paper at: <https://www.>

408 Correspondence and requests should be addressed to A.H or G.R.

409